High-speed operation of GaN/AlGaN quantum cascade detectors at $\lambda \approx 1.55$ μm

A. Vardi,[1,3] N. Kheirodin,[1] L. Nevou,[1] H. Machhadani,[1] L. Vivien,[1] P. Crozat,[1] M. Tchernycheva,[1] R. Colombelli,[1] F. H. Julien,[1,a)] F. Guillot,[2] C. Bougerol,[2] E. Monroy,[2] S. Schacham,[4] and G. Bahir[3]

[1]*Institut d'Electronique Fondamentale, CNRS UMR 8622, Université Paris-Sud XI, 91405 Orsay, France*
[2]*Equipe Mixte, CEA-CNRS-UJF, Nanophysique et Semiconducteurs, DRFMC/SP2M/PSC, CEA Grenoble, 17 rue des Martyrs, 38054 Grenoble Cedex 9, France*
[3]*Department of Electrical Engineering, Technion-Israel Institute of Technology, Haifa 32000, Israel*
[4]*Department of Electrical and Electronic Engineering, Ariel University Center, Ariel 40700, Israel*

(Received 24 July 2008; accepted 21 October 2008; published online 13 November 2008)

We demonstrate room-temperature, high-speed operation of GaN/AlGaN quantum cascade detectors. The devices are processed as square mesas with 50 Ω coplanar access lines. Frequency response measurements were performed under illumination by a modulated laser diode emitting at $\lambda = 1.55$ μm. The electrical response exhibits a first-order filter frequency response. For 17×17 μm^2 (25×25 μm^2) detectors the -3 dB cutoff frequency is 11.4 GHz (6.5 GHz). S-parameter analysis confirms that the cutoff frequency is extrinsically limited and that the speed of the device can be further increased by reducing the device size. © *2008 American Institute of Physics*. [DOI: 10.1063/1.3021376]

Quantum cascade detectors (QCDs) have emerged as an appealing alternative to quantum well infrared photodetectors (QWIPs).[1] In both kinds of devices, the detection relies on photon absorption by electronic intersubband transition in a semiconductor quantum well (QW). The device operating wavelength can be tuned through a wide spectral range by proper choice of the QW thickness. In contrast to QWIPs, QCDs are photovoltaic devices and they can be operated at zero bias. Under illumination, electrons from the ground state are excited to the upper state of the active QW and then transferred to an extractor region where they experience multiple relaxation toward the next active QW. This results in a macroscopic photovoltage in an open circuit configuration, or in a photocurrent if the device is loaded on a resistor. As a major advantage, the dark current is extremely low, which is particularly favorable to enhance the signal-to-noise ratio.[2] QCDs have been demonstrated in several material systems, namely, GaAs/AlGaAs, InGaAs/InAlAs, and InGaAs/AlAsSb, operating at wavelengths in the range of 2.1–84 μm.[3–7] Another appealing feature of QCDs is their intrinsic low capacitance, which enables high frequency response. Cutoff frequencies of ~ 4 GHz at -3 dB have been measured for 100×100 μm^2 InGaAs/InAlAs QCDs.[8]

Recently, we reported on another type of QCD detector in the GaN/AlGaN material system.[9] It makes use of the internal polarization inherent in wurtzite-phase nitride heterostructures for the design of the extractor region. Due to the large conduction band offset at the GaN/AlN interface,[10] the device operates at short near-infrared wavelengths in the range of 1.48–2 μm. The peak responsivity at room temperature is ~ 10 mA/W (~ 1000 V/W) at $\lambda = 1.7$ μm.

In this work, we have investigated the frequency response of GaN/AlGaN QCDs. The devices are processed in the form of square mesas with 50 Ω coplanar access lines for the top and bottom metallic contacts. The optical response was investigated by measuring the photocurrent at $\lambda = 1.55$ μm under illumination of the mesa surface by a rf-modulated laser diode. The frequency response is that of a first-order *RC* filter with cutoff frequencies of 11.4 and 19.7 GHz at -3 dB for 25×25 and the 17×17 μm^2 mesa detectors, respectively. Based on estimates of the intrinsic mechanism limiting time, speed in excess of 80 GHz could be achieved by reducing the device size.

The device was grown by plasma-assisted molecular-beam epitaxy on an AlN/*c*-sapphire pseudosubstrate. It consists of a 40 period active region sandwiched between two *n*-doped (carrier concentration, $n \sim 1 \times 10^{19}$ cm^{-3}) $Al_{0.25}Ga_{0.75}N$ contact layers with a thickness of 500 (200) nm for the bottom (top) layer. Details on the growth procedure can be found in Ref. 9. One period of the active region consists of a *n*-doped 1.5 nm thick GaN QW coupled to an $Al_{0.25}Ga_{0.75}N$/AlN (1/1 nm) multiple QW extractor region. The inset in Fig. 1 shows the conduction band profile of one period of the QCD structure. Upon TM-polarized irradiation, electrons are promoted to the excited state of the GaN QW and then transferred to the QW in the following period via cascaded longitudinal-optical-phonon relaxation through the bound states of the extractor. As a result, a photovoltage is generated across the structure. As shown in Fig. 1, the absorption spectrum exhibits three peaks at 0.66, 0.72, and 0.8 eV, which are attributed to the intersubband absorption of GaN wells with thicknesses of 7, 6, and 5 ML, respectively.[9,10] In turn, the photovoltage spectrum shows a pronounced peak, which corresponds to 6 ML thick QWs (see Fig. 1), suggesting a better transfer of electrons into the extractor. Indeed, as seen in the inset of Fig. 1, the energy separation between the excited state of the 6 ML thick absorbing well and the state confined in the first extractor QW is close to the LO-phonon energy (92 meV) resulting in enhanced scattering. For 5 ML thick QWs this energy separation is of the order of 390 meV, while for 7 ML thick QWs

a)Author to whom correspondence should be addressed. Electronic mail: francois.julien@u-psud.fr.

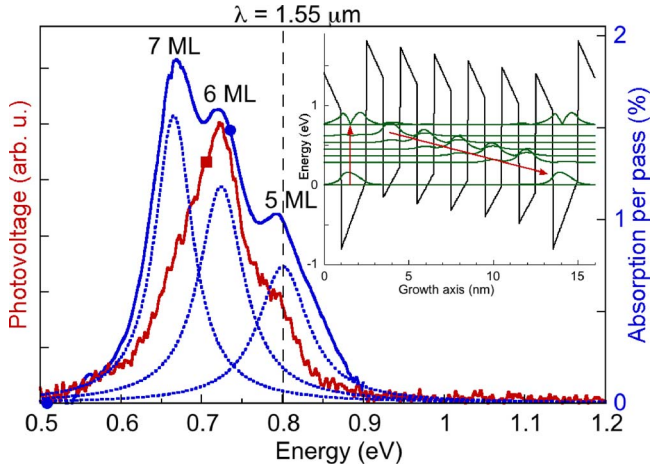

FIG. 1. (Color online) Room-temperature absorption spectrum for one pass through the active region (circles) and photovoltage spectrum (squares). The dotted curves are Lorentzian fits of the absorption for 5, 6, and 7 ML wells. The inset shows the conduction band profile, energy levels, and squared envelope functions of one period of the QCD structure with 6 ML thick GaN wells calculated using an eight-band $\mathbf{k}.\mathbf{p}$ model.

the state confined in the first extractor QW is at a higher energy than that of the active well excited state, both situations resulting in a lower transfer efficiency with respect to the 6 ML thick QWs.[9] Incidentally, the fact that in our device the photovoltage is maximum for 6 ML and not 7 ML wells excludes any significant contribution from an optical rectification process.[11] Finally, it should be noted that the photoresponse at $\lambda = 1.55$ μm mainly arises from 5 ML thick QWs.

The detectors are processed in the form of square 17 $\times$ 17 and 25 $\times$ 25 μm^2 mesas with hollow top contacts in order to allow illumination from their surface. They are electrically contacted using 50 Ω coplanar access lines. The inset of Fig. 2 shows a scanning electron microscope image of a 17 $\times$ 17 μm^2 mesa QCD. The device fabrication relies on two consecutive etching steps. The first etch down to the bottom AlGaN layer is used to fabricate the mesas and allow for bottom contacting (region C in Fig. 2). A second etch down to the sapphire substrate is then performed to remove the doped AlGaN layer under the access lines (region A in Fig. 2). The etching was performed in an ICP-RIE system

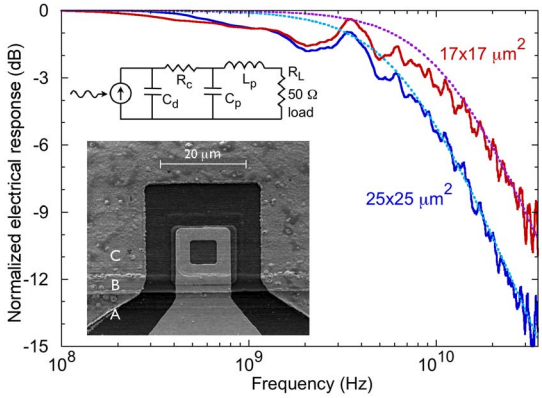

FIG. 2. (Color online) Normalized electrical response in dB at room temperature of the QCD vs modulation frequency for 25 $\times$ 25 and 17 $\times$ 17 μm^2 mesas. The full (dotted) curves are the measurements (simulations). The top inset shows the equivalent electrical circuit. The bottom inset is a scanning electron microscope image of one mesa detector.

TABLE I. Equivalent electrical circuit parameters of the QCD deduced from S-parameter analysis. C_d is the device capacitance, R_c is the access resistance, C_p is the parasitic capacitance, L_p is the parasitic inductance, and R_L is the 50 Ω load resistance. The standard deviations are 10 fF and 40 Ω for C_d and R_c, respectively.

Size (μm)	R_c (Ω)	C_d (fF)	L_p (pH)	C_p (fF)
17	210	45	59	24
25	180	97	63	27

using a dielectric SiO_2 mask and a Cl_2/Ar plasma. After the etching steps, the mesas were isolated via a Si_3N_4 deposition (region B in Fig. 2). A Ti/Al/Ti/Au (5/25/15/100 nm) metallization was then performed. The bottom contact was annealed at 650 °C and presents an Ohmic behavior with a specific contact resistivity of 2×10^{-4} Ω cm^2.

The photocurrent responsivity was measured in the 0.1–50 GHz frequency range with the device loaded on a 50 Ω resistor using an Agilent 86030A lightwave component analyzer (LCA). TM-polarized light excitation was provided by a continuous-wave laser diode at $\lambda = 1.55$ μm. The light was modulated at rf frequencies by a lithium niobate modulator driven by the LCA and further amplified using an erbium doped fiber amplifier. A polarization-maintaining lens fiber was used to illuminate the surface of the QCD mesas at 45° angle of incidence. Microwave probes adapted up to 50 GHz were connected to the coplanar access lines linked to the top and bottom contacts. Autocalibration of the test bench optical modulator was carried out up to 50 GHz.

Figure 2 shows the room-temperature electrical response (20 log[photocurrent]) in dB of the 25 $\times$ 25 and 17 $\times$ 17 μm^2 mesa detectors as a function of the modulation frequency. The curves have been normalized at 0 dB at low frequencies. Apart from some instrument-related artifacts around 1–3 GHz, the frequency response of the detectors resembles that of a first-order *RC* filter with a slope at high frequencies of 20 dB/decade. The −3 dB cutoff frequency is 6.5 GHz for the 25 $\times$ 25 μm^2 detectors and 11.4 GHz for the 17 $\times$ 17 μm^2 detectors. At low frequencies, the responsivity of the various mesa detectors at $\lambda = 1.55$ μm is measured to be in the range of 2–2.5 mA/W. It should be noted that this experimental value of the responsivity is one order of magnitude larger than the theoretical estimates,[5] assuming 1.1% absorption probability per one pass through the QCD stack and $N_p = 40$ periods. We suspect that this surprising enhancement of the responsivity is related to the thickness monolayer fluctuations of the thin GaN QWs and that one should consider a reduced number of periods to calculate the responsivity.

The frequency response of the QCD can be understood considering its rf equivalent circuit shown in the inset of Fig. 2. In this scheme we assume that the QCD behaves as a current source, C_d is the device capacitance, R_c is the access resistance due to the metal contacts and to the resistivity of the AlGaN contact layers, C_p is the parasitic capacitance between the top and bottom contacts, and L_p is the parasitic inductance probably resulting from the junction between the top contact and the access line. The equivalent-circuit elements were extracted by measurement of the S-parameters of the devices using a 50 GHz network analyzer. Table I summarizes the averaged values deduced from measurements

performed on six different devices. Simulations using the values in Table I show that C_p and L_p would only have a significant impact on the performance at frequencies larger than 150 GHz, i.e., well beyond the currently investigated frequency range. The limiting parameter is the device capacitance C_d, which is in the order of 97 ± 10 fF for the 25×25 μm^2, in good agreement with the theoretical estimation of 105 fF, calculated taking into account the total active region thickness and using a dielectric constant of 8.5 (8.8) ε_0 for AlN ($Al_{0.25}Ga_{0.75}N$).[12,13] Comparing the two sizes of mesas, C_d roughly scales linearly with the mesa surface area within the error bars. In contrast, the contact resistance increases when the mesa size is reduced.

Neglecting the parasitic inductance and capacitance, the photocurrent circulating in the load resistor can be approximated as

$$i = I/\sqrt{1 + 4\pi^2 f^2 \tau^2},$$

where f is the frequency and the time constant is given by $\tau = (R_c + R_L) \times C_d$. The simulated optical response is that of a first-order filter with a −3 dB cutoff frequency $f_c = 1/(2\pi\tau)$. The dotted curves in Fig. 2 show the fitted optical response for the two sizes of mesa detectors. The best fit is achieved using $\tau = 24.5$ ps and $\tau = 14$ ps for the 25×25 and 17×17 μm^2 mesas, respectively. These values are in good agreement with the time constants estimated from the values listed in Table I, $\tau = 22 \pm 7$ ps and $\tau = 12 \pm 5$ ps, respectively.

It should be noted that the agreement between simulations and measurements of the optical response, and especially the fact that f_c scales with the device area, demonstrates that the speed of the QCDs is governed by the *RC* filter and not by an intrinsic mechanism. The latter mechanism is the transport time of electrons within the active region. This mechanism should manifest itself as a 40 dB/decade slope of the optical response at large enough frequencies (second-order filter), which is not observed in the experimental measurements within the investigated frequency range. Therefore, we can conclude that intrinsic limitations occur at frequencies above 30 GHz, which gives an upper estimate of the electron transport time of about 5 ps. Considering the energy level diagram, the main intrinsic factor limiting the transport time should be the nonresonant tunneling time, τ_t, between the active 5 ML thick QW and the first extractor QW. Indeed, the relaxation of electrons in the extractor should be extremely fast since the energy spacing between the adjacent QW states of the extractor (≈ 100 meV) is close to the energy of the LO-phonon. The lifetime of electrons in the excited state of the active QW is limited by two competing mechanisms: the intersubband relaxation to the ground state and the nonresonant tunneling into the extractor, which gives rise to the photocurrent. Therefore, the nonresonant tunneling time can be estimated as $\tau_t \approx \tau_{21} \times (1/\eta_i - \eta_i)$, where τ_{21} is the intersubband relaxation time and η_i is the internal quantum efficiency, i.e., the number of electrons generated in the external circuit per absorbed photon, given by $\eta_i = (h\nu/e) \times (R/a) \approx 0.14$, where $h\nu = 0.8$ eV is the photon energy, e is the electron charge, and $R \approx 2$ mA/W and $a \approx 1.1\%$ are the responsitivity and the absorption per pass at $\lambda = 1.55$ μm, respectively. Based on the value $\tau_{21} \approx 140$ fs recently measured for an intersubband transition at $\lambda = 1.5$ μm in GaN/AlN QWs,[14] the nonresonant tunneling time is deduced to be $\tau_t \approx 1$ ps. We estimate that the total transport time should be <2 ps, which corresponds to an intrinsic cutoff frequency of >80 GHz. In order to test the intrinsic speed of the QCD, the device dimensions must be reduced. One possible design would be to fabricate a 2×10 μm^2 waveguide detector in order to benefit from both high speed and enhanced responsivity.

In conclusion, we have demonstrated the room-temperature, high-speed operation of QCDs based on GaN/AlGaN QWs. The −3 dB cutoff frequency of the electrical response is measured to be as high as 11.4 GHz for 17×17 μm^2 mesa detectors, which is a factor of 3 larger than the previously reported measurements on InGaAs/AlInAs QCDs.[8] Cutoff frequencies in excess of 80 GHz could be obtained by further reducing the size of the devices.

We acknowledge fruitful discussions with V. Berger. The AlN/*c*-sapphire substrates were provided by DOWA Electronics Materials, Inc. This work was supported in part by ANR-06-BLAN-0130 TRANSNIT and by the U.S.-Israel Binational Science Foundation under Contract No. 2004366.

[1] L. Gendron, M. Carras, A. Huynh, V. Ortiz, C. Koeniguer, and V. Berger, Appl. Phys. Lett. **85**, 2824 (2004).
[2] A. Gomez, N. Péré-Laperne, L.-A. de Vaulchier, C. Koeniguer, A. Vasanelli, A. Nedelcu, X. Marcadet, Y. Guldner, and V. Berger, Phys. Rev. B **77**, 085307 (2008).
[3] L. Gendron, C. Koeniguer, V. Berger, and X. Marcadet, Appl. Phys. Lett. **86**, 121116 (2005).
[4] M. Graf, N. Hoyler, M. Giovannini, J. Faist, and D. Hofstetter, Appl. Phys. Lett. **88**, 241118 (2006).
[5] F. R. Giorgetta, E. Baumann, M. Graf, L. Ajili, N. Hoyler, M. Giovannini, J. Faist, D. Hofstetter, P. Krotz, and G. Sonnabend, Appl. Phys. Lett. **90**, 231111 (2007).
[6] M. Graf, G. Scalari, D. Hofstetter, J. Faist, H. Beere, E. Linfield, D. Ritchie, and G. Davies, Appl. Phys. Lett. **84**, 475 (2004).
[7] F. R. Giorgetta, E. Baumann, D. Hofstetter, C. Manz, Q. Yang, K. Köhler, and M. Graf, Appl. Phys. Lett. **91**, 111115 (2007).
[8] D. Hofstetter, M. Graf, T. Aellen, J. Faist, L. Hvozdara, and S. Blaser, Appl. Phys. Lett. **89**, 061119 (2006).
[9] A. Vardi, G. Bahir, F. Guillot, C. Bougerol, E. Monroy, S. E. Schacham, M. Tchernycheva, and F. H. Julien, Appl. Phys. Lett. **92**, 011112 (2008).
[10] M. Tchernycheva, L. Nevou, L. Doyennette, F. H. Julien, E. Warde, F. Guillot, E. Monroy, E. Bellet-Amalric, T. Remmele, and M. Albrecht, Phys. Rev. B **73**, 125347 (2006).
[11] D. Hofstetter, E. Baumann, F. R. Giorgetta, F. Guillot, S. Leconte, and E. Monroy, Appl. Phys. Lett. **91**, 131115 (2007).
[12] S. N. Mohammad and H. Morkoc, Prog. Quantum Electron. **20**, 361 (1996).
[13] V. W. L. Chin, T. L. Tansley, and T. Osotchan, J. Appl. Phys. **75**, 7365 (1994).
[14] J. Hamazaki, S. Matsui, H. Kunugita, K. Ema, H. Kanazawa, T. Tachibana, A. Kikuchi, and K. Kishino, Appl. Phys. Lett. **84**, 1102 (2004).